Nanoporous, Honeycomb-Structured Network Fibers Spun from Semiflexible, Ultrahigh Molecular Weight, Disubstituted Aromatic Polyacetylenes: Superhierarchical Structure and Unique Optical Anisotropy

Giseop Kwak,*[,†,‡] Satoshi Fukao,[‡] Michiya Fujiki,*[,‡] Toshikazu Sakaguchi,[§] and Toshio Masuda[§]

Department of Polymer Science, Kyungpook National University, 1370 Sankyuk-dong, Buk-ku, Daegu 702-701, Korea, Graduate School of Materials Science, Nara Institute of Science and Technology, 8916-5 Takayama, Ikoma, Nara 630-0101, Japan, and Department of Polymer Chemistry, Graduate School of Engineering, Kyoto University, Katsura Campus, Kyoto 615-8510, Japan

Received July 24, 2006. Revised Manuscript Received September 18, 2006

A diaryl-substituted polyacetylene, poly[1-(trimethylsilyl)phenyl-2-phenylacetylene] (**PTMSDPA**), provided nanoporous, honeycomb-structured network fibers by electrospinning the chloroform solution with about 1.6 wt % polymer. The **PTMSDPA** fibers formed a nanoporous, honeycomb-network structure. These fibers emitted an intense yellowish green light. The main axis of yellowish green emission in the fiber appeared to be perpendicular to the fiber axis. The polarization ratio ($I_{\perp}/I_{\parallel}$) in fluorescence (FL) attained a value of ~4.7 and the FL peak band of the perpendicular axis (λ_{max} = 548 nm) was slightly red-shifted by 9 nm compared to that of the parallel one (λ_{max} = 539 nm). The ultrahigh M_w of 8.0×10^5 and the relatively high α value of 0.765 were responsible for the lyotropic liquid crystallinity of **PTMSDPA**. The weak charge separation within the repeat unit of **PTMSDPA** was assumed to be responsible for the unique optical anisotropy of strong emission perpendicular to the fiber axis.

Introduction

The most notable fiber spinning approach might be a modern electrospinning technique that is now acknowledged to be one of the most versatile fabrication methods for simple preparation of various functional fibers of nanometer size. The technique has several advantages including low cost, easy setup, and a high-throughput continuous production process, allowing one to make functional nanofibers from a wide range of synthetic polymers and ceramics.[1] The electrospun nanofibers have many practical applications as parts of free-standing porous membrane filters with ultrahigh permeability, external-stimuli-responsive drug delivery systems, and sensory devices with ultrahigh sensitivity and selectivity because of their intrinsically high surface area-to-volume ratio. Recently, electrospun nanofibers made of π-conjugating and/or semiconducting polymers received much attention in the fields of molecular electronics and photonics.[2−11] This is because photoexcited electron−hole (*e*−*h*) pairs and free carriers would be effectively confined in the nanospaces of the quasi-one-dimensional (1D) semiconducting nanofibers. The photophysical and electrical properties of nanofibers may be very different from those of bulk films made of the same constituents. However, high precision in controlling all molecular orientations, morphologies, and alignments of the fibers is required to afford unique functions and applications of 1D polymers in spun fibers.[12]

Currently, there are many kinds of π-conjugating polymers synthesized by metal-catalyzed cross-coupling reactions including poly(phenylene)s, poly(phenylenevinylene)s, and poly(phenyleneethylene)s.[13−16] As most of these π-conjugating polymers are nonpolar and/or less polar and their molecular weights are limited to a range of only 10^3−10^4, it

* Authors to whom correspondence should be addressed. E-mail: gkwak@knu.ac.kr (G.K.); fujikim@ms.naist.jp (M.F.).
† Kyungpook National University.
‡ Nara Institute of Science and Technology.
§ Kyoto University.

(1) For a recent review, see: Li, D.; Xia, Y. *Adv. Mater.* **2004**, *16*, 1151−1170.
(2) Jang, S.-Y.; Seshadri, V.; Khil, M.-S.; Kumar, A.; Marquez, M.; Mather, P. T.; Sotzing, G. A. *Adv. Mater.* **2005**, *17*, 2177−2180.
(3) Babel, A.; Li, D.; Xia, Y.; Jenekhe, S. A. *Macromolecules* **2005**, *38*, 4705−4711.
(4) Li, D.; Babel, A.; Jenekhe, S. A.; Xia, Y. *Adv. Mater.* **2004**, *16*, 2062−2066.
(5) Yu, J. H.; Fridrikh, S. V.; Rutledge, G. C. *Adv. Mater.* **2004**, *16*, 1562−1566.
(6) Sun, Z.; Zussman, E.; Yarin, A. L.; Wendorff, J. H.; Greiner, A. *Adv. Mater.* **2003**, *15*, 1929−1932.
(7) Madhugiri, S.; Dalton, A.; Gutierrez, J.; Ferraris, J. P.; Balkus, K. J. *J. Am. Chem. Soc.* **2003**, *125*, 14531−14538.
(8) MacDiarmid, A. G.; Jones, W. E.; Norris, I. D.; Gao, J.; Johnson, A. T.; Pinto, N. J.; Hone, J.; Han, B.; Ko, F. K.; Okuzaki, H.; Llaguno, M. *Synth. Met.* **2001**, *119*, 27−30.
(9) Chen, Z.; Foster, M. D.; Zhou, W.; Fong, H.; Reneker, D. H.; Resenders, R.; Manners, I. *Macromolecules* **2001**, *34*, 6156−6158.
(10) Okuzaki, H.; Ishihara, M. *Macromol. Rapid Commun.* **2003**, *24*, 261−264.
(11) Okuzaki, H.; Takahashi, T.; Miyajima, N.; Suzuki, Y.; Kuwabara, T. *Macromolecules* **2006**, *39*, 4276−4278.
(12) Dersch, R.; Liu, T.; Schaper, A. K.; Greiner, A.; Wendorff, J. H. *J. Polym. Sci., Part A: Polym. Chem.* **2003**, *41*, 545−553.
(13) Miyaura, N.; Suzuki, A. *Chem. Rev.* **1995**, *95*, 2457−2483.
(14) Stille, J. K. *Angew. Chem., Int. Ed. Engl.* **1986**, *25*, 508−524.
(15) Heck, R. F. *Org. React.* **1982**, *27*, 345−390.
(16) Sonogashira, K. In *Metal-Catalyzed Cross-Coupling Reactions*; Diederich, F., Stang, P. J., Eds.; Wiley-VCH: New York, 1998; Chapter 5.

10.1021/cm061719u CCC: $33.50
Published on Web 10/24/2006

Chart 1. Chemical Structure of PTMSDPA

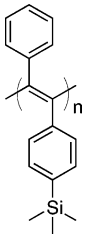

is very difficult to obtain electrospun fibers by an ordinary electrospinning method. As for such lower weight-average molecular weight (M_w) polymers, very special electrospinning methods, such as the coaxial, two-capillary spinneret method,[3−6] the blending method,[7,17,18] and precursor method,[2,11] are inevitably required.

In contrast, disubstituted acetylene polymers with ultrahigh M_w can be readily obtained the group 5 transition metal catalysts such as $TaCl_5$ and $NbCl_5$.[19] Disubstituted aromatic acetylene polymers obtained by the $TaCl_5-n$-Bu_4Sn catalyst are typical examples.

Among these polymers, poly[1-(trimethylsilyl)phenyl-2-phenylacetylene] (**PTMSDPA**, in Chart 1), possesses several unique qualities including (a) an ultrahigh M_w of ca. 1×10^6, (b) excellent chemical and mechanical stability,[20,21] (c) a semiflexible main chain bearing two bulky aryl side groups, (d) high solubility in common organic solvents such as chloroform and THF, (e) an extremely high viscosity even in low concentration less than 1.0 wt % due to the semiflexible conformation and ultrahigh M_w, (f) an intense fluorescence in green color, and (g) considerable polarity perpendicular to the main direction, but less polarity parallel to the main direction. One can expect that these excellent properties of **PTMSDPA** enable us to prepare highly luminous electrospun nanofibers by a conventional electrospinning method.

In this paper, the authors use an ultrahigh M_w **PTMSDPA** sample to demonstrate the first successful preparation and unique morphological structures of hierarchical nanoporous electrospun fibers exhibiting a high optical anisotropy. This knowledge and understanding may lead to a new approach in easily exploring highly polarized device materials such as an electroluminescent (EL) device,[22,23] optical sensor,[24] and fluorescence image patterning.[25]

Results and Discussion

The **PTMSDPA** used in this study was donated by NOF Corporation (Tokyo, Japan). The M_w and molecular weight distribution (M_w/M_n) determined by gel permeation chromatography were estimated to be 8.0×10^5 and 1.8, respectively. Solution properties, controlled variables, and ambient parameters in the electrospinning process can significantly influence the morphology of the resultant polymer nanofibers. The authors first examined the individual influences of solvent, concentration, applied voltage, tip-to-collector distance, and feed rate on the processability of nanofibers of **PTMSDPA**. The solvent property and the concentration of the solution were found to strongly influence the processability, as described below.

First, this polymer formed fibril structures from both chloroform and THF solutions under an appropriate condition, but not from toluene solution. Chloroform (dielectric constant, $D = 4.8$ at 20 °C) and THF (7.4) are more polar than toluene (2.3), allowing an electric field to be applied to the droplets of the solutions with comparative ease. Second, the influence of the concentration of chloroform and THF was tested. The formation of fibers increased to the maximum by increasing the concentration up to 1.62 wt %, as shown in Figure 1. However, this polymer did not dissolve any more in concentrations higher than 1.62 wt % and turned to a gel. It was thus impossible to further test the effect of concentration. Parameters other than solvent and concentration had little influence on the morphology of the **PTMSDPA** fiber. Accordingly, all subsequent spectroscopic and microscopic measurements were conducted by using fiber that was spun from the 1.62 wt % polymer solution in chloroform applied with 18 kV at a tip-to-collector distance of 15 cm, unless otherwise noted.

Figure 2 shows the fluorescence optical microscope (OM) and magnified scanning electron microscope (SEM) images of electrospun **PTMSDPA** fibers. The fluorescence image of **PTMSDPA** excited at 365 nm shows that fibers several micrometers in diameter emitted an intense yellowish green color. In the magnified SEM image, **PTMSDPA** fibers formed a porous network structure with a honeycomb-like pattern. Such porous hierarchical morphology of the electrospun fiber is basically ascribed to a phase separation induced by the rapid evaporation of solvents with lower boiling points and a subsequent rapid solidification during the electrospinning process.[26,27] Also, the honeycomb pattern of the fiber should be due to the atmospheric humidity, resulting from a template which consists of water microspheres during the evaporation of the polymer solution.[28,29] To our knowledge, this may be the first example of

(17) Wutticharoenmongkol, P.; Supaphol, P.; Shikhirin, T.; Kerdchroen, T.; Osotchan, T. *J. Polym. Sci., Part B: Polym. Phys.* **2005**, *43*, 1881−1891.
(18) Wei, M.; Lee, J.; Kang, B.; Mead, J. *Macromol. Rapid Commun.* **2005**, *26*, 1127−1132.
(19) For reviews of substituted polyacetylenes, see: (a) Masuda, T.; Sanda, F. In *Handbook of Metathesis*; Grubbs, R. H., Ed.; Wiley-VCH: Weinheim, 2003; Vol. 3, Chapter 3, p 11, 2003. (b) Nomura, R.; Masuda, T. In *Encyclopedia of Polymer Science and Technology*; Kroshwitz, J. I., Ed.; Wiley: New York, 2003; Vol. IA.
(20) Tsuchihara, K.; Masuda, T.; Higashimura, T. *J. Am. Chem. Soc.* **1991**, *113*, 8548−8549.
(21) Tsuchihara, K.; Masuda, T.; Higashimura, T. *Macromolecules* **1992**, *25*, 5816−5820.
(22) Hidayat, R.; Hirohata, M.; Tatsuhara, S.; Ozaki, M.; Yoshino, K.; Teraguchi, M.; Masuda, T. *Synth. Met.* **1999**, *101*, 210−211.
(23) Yoshino, K.; Hirohata, M.; Hidayato, R.; Kim, D. W.; Tada, K.; Ozaki, M.; Teraguchi, M.; Masuda, T. *Synth. Met.* **1999**, *102*, 1159.
(24) Liu, Y.; Mills, R. C.; Boncella, J. M.; Schanze, K. *Langmuir* **2001**, *17*, 7452−7455.
(25) Kwak, G.; Fujiki, M.; Sakaguchi, T.; Masuda, T. *Macromolecules* **2006**, *39*, 319−323.
(26) Bognizki, M.; Czado, W.; Frese, T.; Schaper, A.; Hellwig, M.; Steinhart, M.; Greiner, A.; Wendorff, J. H. *Adv. Mater.* **2001**, *13*, 70−72.
(27) Megelski, S.; Stephens, J. S.; Chase, D. B.; Rabolt, J. F. *Macromolecules* **2002**, *35*, 8456−8466.
(28) Karthaus, O.; Maruyam, N.; Cleren, X.; Shimomura, M.; Hasegawa, H.; Hashimoto, T. *Langmuir* **2000**, *16*, 6071−6076.
(29) Yabu, H.; Tanaka, M.; Ijiro, K.; Shimomura, M. *Langmuir* **2003**, *19*, 6297−6300.

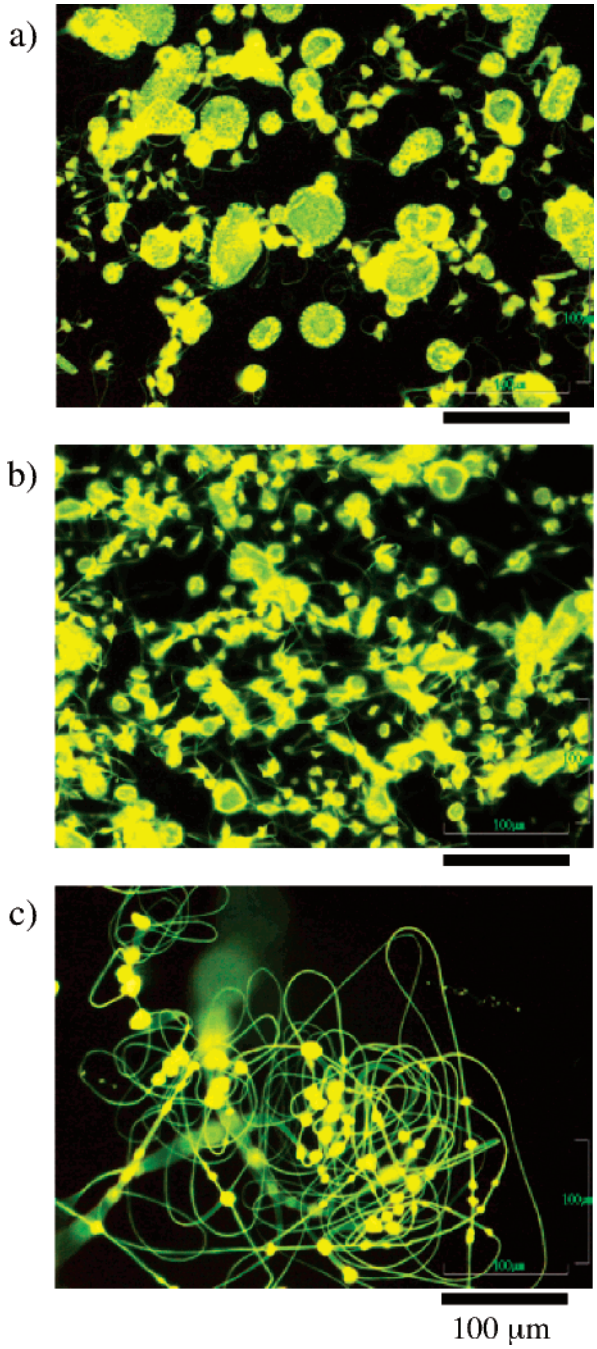

Figure 1. Fluorescence optical microscope images of **PTMSDPA** electrospun fibers prepared from chloroform solution of (a) 0.73 wt %, (b) 1.07 wt %, and (c) 1.62 wt %.

honeycomb structure of conjugating polymer in an electrospun fiber.

Figure 3 shows polarized fluorescence (FL) images of **PTMSDPA** fiber excited at 365 nm by an unpolarized UV light source. The main axis of yellowish green emission in the fiber appeared to be perpendicular to the fiber axis, but not parallel. This polarized FL spectra of the **PTMSDPA** fiber is shown in Figure 4. Indeed, the intensity and emission-peak wavelength in the FL spectra around 540−550 nm changed significantly with the polarizer direction. The polarization ratio ($I_{\perp}/I_{\parallel}$) in FL attains a value of ∼4.7 and the FL peak band of the perpendicular axis ($\lambda_{max} = 548$ nm) is slightly red-shifted by 9 nm compared to that of the parallel one ($\lambda_{max} = 539$ nm). Because these emissions come from

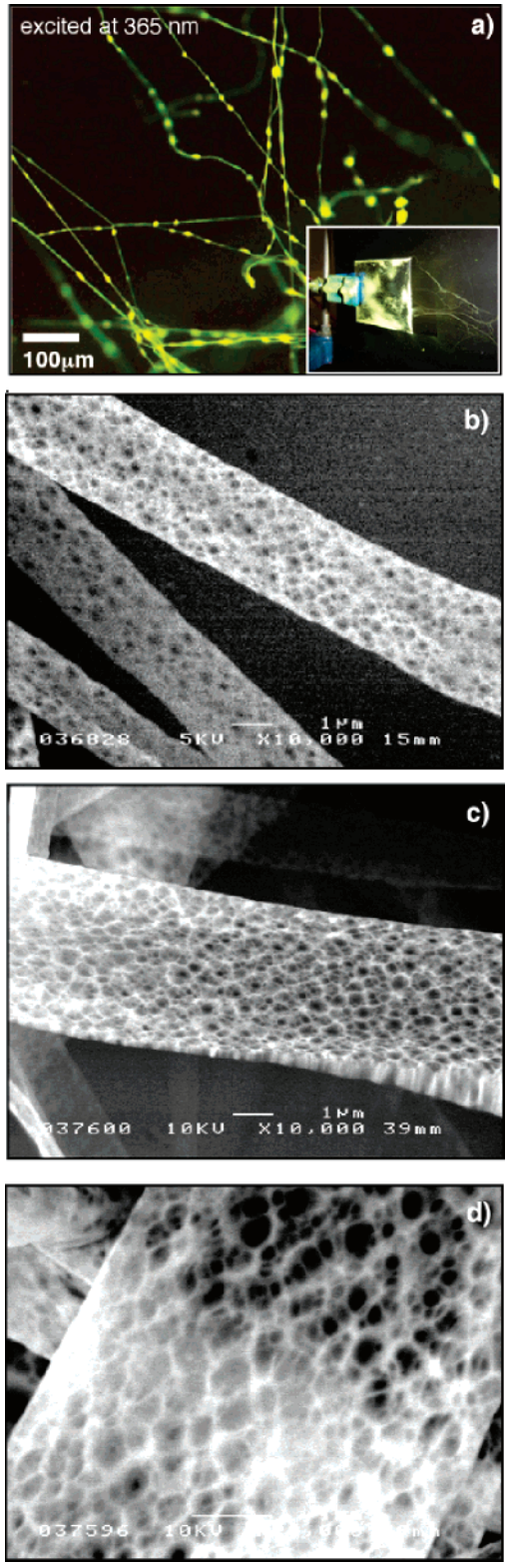

Figure 2. (a) Fluorescent optical microscope images (insert: photograph of the nonwoven mat collected on ITO-PEN); SEM images of electrospun fibers of **PTMSDPA** magnified by (b) 5×10^3, (c) 1×10^4, and (d) 2×10^4 times.

the main chain axis of **PTMSDPA**, the aligned main chains are highly elongated and densely packed, leading to longer conjugation lengths. The present result is in sharp contrast to previously accepted theory that the main chain axis of linear polymer chains prefers to orient parallel to the fiber axis due to strong stretching and shearing forces of the

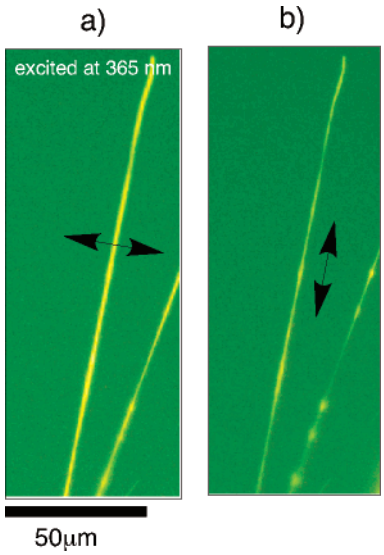

Figure 3. Fluorescent optical microscope images of a single nanofiber with (a) perpendicular and (b) parallel arrangements to the direction of a linear polarizer, respectively. The arrow indicates the direction of the polarizer.

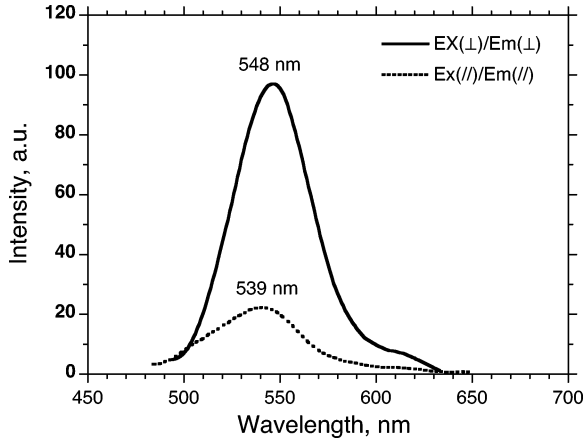

Figure 4. Polarized fluorescence spectra of a mechanically aligned fiber mat (λ_{ex} = 375 nm); Ex(⊥), Em(⊥), Ex(||), and Em(||) refer to the perpendicular excitation, perpendicular emission, parallel excitation, and parallel emission to the aligned direction of the mat, respectively.

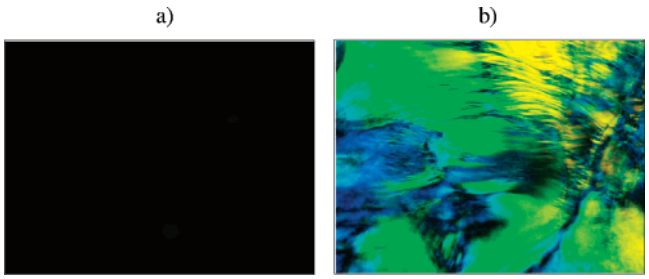

Figure 5. Polarized optical microscope images of 1.62 wt % **PTMSDPA** in chloroform (a) before and (b) after evaporation.

polymer liquid jet during electrospinning. The **PTMSDPA** electrospun nanofiber described here is thus unique and is a very rare example because the main chain axis of **PTMSDPA** is actually aligned perpendicular to the fiber axis.

To elucidate the origin of the FL anisotropy for **PTMSDPA** fiber, we examined changes in the lyotropic liquid crystallinity of the polymer solution in chloroform caused by increasing the polymer concentration. Figure 5 shows the polarized microscope images of the 1.62 wt % chloroform solution of **PTMSDPA**. Although the polymer solution in

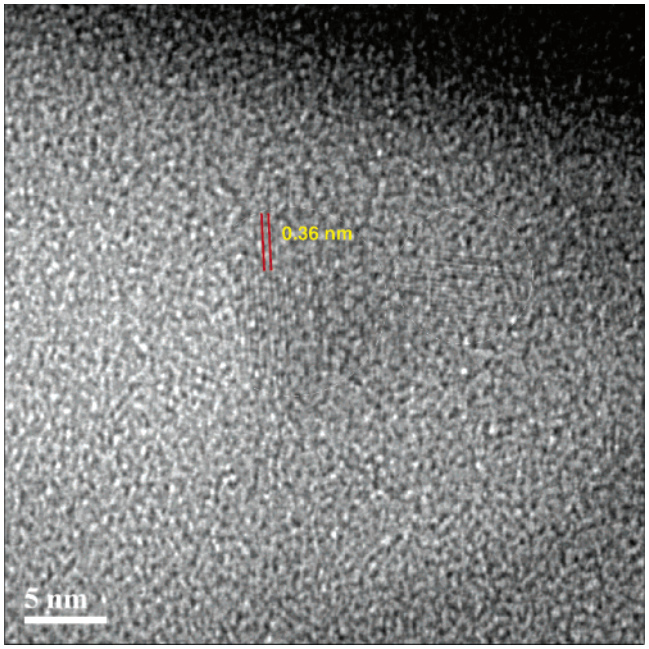

Figure 6. High-resolution TEM image of **PTMSDPA** fiber after annealing at 200 °C for 1 h.

the electrospinning experiments was completely isotropic, the solution generated an intense optical birefringence above a certain critical concentration ($[conc]_c$) by slowly evaporating the polymer solution. With further evaporation, the solution underwent a gelation, resulting in the formation of a solid film. This birefringence indicates formation of liquid crystalline phases in the solution of **PTMSDPA**. It has been proved theoretically and experimentally that, in the case of a semiflexible polymer in solution, (a) when the polymer concentration exceeded its critical value of $[conc]_c$, polymer chains can become spontaneously self-organized, leading to lyotropic liquid crystals through an isotropic liquid crystal phase transition,[30,31] and (b) as the value of M_w of the semiflexible polymer increases, the value of $[conc]_c$ decreases. Indeed, the semiflexible nature of **PTMSDPA** was evident from the relatively high viscosity index of $\alpha = 0.765$ ($3.0 \times 10^5 < M < 2.8 \times 10^6$ in THF at 40 °C). This was obtained by $[\eta] = KM^{\alpha}$ from the Mark−Houwink−Sakurada plot using a universal calibration curve, where $[\eta]$ and M are the intrinsic viscosity and absolute molecular weight, respectively. Also, as previously mentioned, the molecular weight of **PTMSDPA** was extremely high. The values of ultrahigh M_w and the α characteristic of **PTMSDPA** should be responsible for the lyotropic liquid crystallinity. Thus, the optical anisotropy of **PTMSDPA** fiber originates from the lyotropic liquid crystallinity induced by solvent evaporation in the process of electrospinning.

Such a semiflexible polymer tends to lower its entropy energy by densely packing the chains via intermolecular interactions, resulting in liquid crystalline phases. Figure 6 shows the high-resolution transmission electron microscope (TEM) image of **PTMSDPA** nanofiber annealed at 200 °C for 1 h. This fiber exhibited several domains with certain

(30) Sato, T.; Teramoto, A. *Adv. Polym. Sci.* **1996**, *126*, 85−161.
(31) Natsume, T.; Wu, L.; Sato, T.; Terao, K.; Teramoto, A.; Fujiki, M. *Macromolecules* **2001**, *34*, 7899−7904.

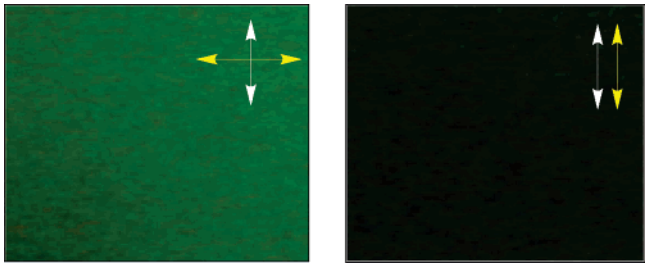

Figure 7. Polarized fluorescent optical microscope images of **PTMSDPA** film solidified after rubbing the solution (white and yellow arrows indicate directions of rubbing and polarizer, respectively).

lattice fringes of *d*-space of ~3.6 Å due to $\pi-\pi$ stacking main chain. Furthermore, such domains increased and grew bigger when the annealing time was inceased. This indicates that the polymer chains in electrospun fibers partly turn to densely packed crystalline structures through thermo-driven reorganization.

The issue of why the **PTMSDPA** polymer chain can be perpendicularly aligned to the fiber axis is a puzzling one. When the polymer solution was sheared after an occurrence of the liquid crystalline phase, the polymer film actually showed the intense polarized FL perpendicular to the shearing direction (see Figure 7). Similar results concerning the perpendicular alignment of semiflexible, liquid crystalline polymers involving disubstituted poly(phenylene)s and poly(phenylenevinylene)s have been reported by Akagi and coworkers.[32] The main chain of **PTMSDPA** is semiflexible. Hence, it can be regarded as a sequence of mesogenic cores. In addition, the stacking structures of such self-assemblies would be determined by certain weak interactions and a subtle balance between the mesogens. At this time, we thus presume that a weak charge separation occurs locally within the repeat unit of the silylenephenylenevinylenephenylene moiety, and the resulting dipole vector is perpendicular to the main chain. In other words, both the semiflexible structure of the backbone and the dipole−dipole interactions would obstruct arrangement of the polymer chain parallel to the sheared direction.

As mentioned above, the superhierarchical morphology and the optical anisotropy of the **PTMSDPA** fiber are very unusual because these phenomena are not explicable in terms of the general idea that the polymer chains in a uniform fiber should align parallel to the fiber axis. Here, we wish to propose a possible orientation mechanism of the electrospinning process of **PTMSDPA**, as shown in Scheme 1: In the first stage, an isotropic liquid crystalline phase transition occurs in the initial period of solvent evaporation. In the second stage, the liquid jet turns to a gel and is strongly stretched with simultaneous alignment of polymer chains perpendicular to the jet axis. Finally, in the third stage, the jet is solidified, resulting in porosity and a honeycomb structure of the fiber.

The present finding and proposed ideas constitute a promising new and simple approach for the next-generation, highly polarized, and/or anisotropic polymeric materials by conventional high-throughput electrospinning processing and

Scheme 1. Proposed Electrospinning Process of the 1.62 wt % PTMSDPA Solution in Chloroform

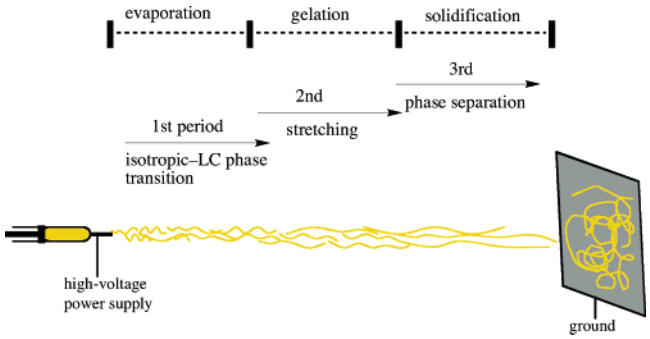

newly programmed conjugating polymers. For example, the large surface areas of the porous structures will give advantages for applications of unique optical sensors with ultrahigh sensitivity and selectivity.[33,34] Furthermore, the FL anisotropy is also applicable to switching in a preferential optical axis in photonic and electronic device materials. This is because the signals of the *e*−*h* pairs and free electron−hole carriers would be confined to superhierarchical networks embedded in nanospaces made of various 1D semiconducting polymers. High precision in controlling molecular orientation, morphology, and alignment of the fibers is also required to allow high-performance functions and applications of 1D polymers in spun fibers.

Conclusion

We successfully prepared electrospun nanoporous fibers using semiflexible diaryl-substituted polyacetylene, poly[1-(trimethylsilyl)phenyl-2-phenylacetylene]. Unique superhierarchical morphological structures such as a honeycomb network were observed. The fibers exhibited a high anisotropy of photoluminescence. Furthermore, the main axis of strong emission was perpendicular to the fiber axis. This polymer had ultrahigh M_w and the relatively high α value, resulting in lyotropic liquid crystalline characteristics. Both the semiflexible structure of the backbone and the weak charge separation within the repeat unit were likely to obstruct arrangement of the polymer chain parallel to the sheared direction.

Experimental Method

In a typical procedure for electrospinning, **PTMSDPA** solution was added to a syringe connected to the metallic needle. The solution was fed by a syringe pump (KDS 100, KD Scientific Inc.). The feed rate for the **PTMSDPA** solution varied in the range of 0.05−0.5 mL/h. The metallic needle was connected to a high-voltage power supply (AKT-030KPS, Towa Keisoku, Tokyo, Japan), and an ITO-PEN film (TOBI, Osaka, Japan) was placed at a suitable distance in the range of 10−20 cm from the tip of the needle to collect the resulting nanofibers. The spinning voltage was set at a voltage in the range of 15−22 kV. The weight-average molecular weight (M_w) and number-average molecular weight (M_n)

(32) Oguma, J.; Kawamoto, R.; Goto, H.; Itoh, K.; Akagi, K. *Synth. Met.* **2001**, *119*, 537−538.

(33) Wang, X.; Drew, C.; Lee, S.-H.; Senecal. K. J.; Kumar, J.; Samuelson, L. A. *Nano Lett.* **2002**, *2*, 1273−1275.

(34) Wang, X.; Kim, Y.-G.; Drew, C.; Ku, B.-C.; Kumar, J.; Samuelson, L. A. *Nano Lett.* **2004**, *4*, 331−334.

of the polymer were evaluated using gel permeation chromatography (Shimadzu A10 instruments (Kyoto, Japan), Polymer Laboratories (Shropshire, UK), PLgel Mixed-B with 300 mm in length as a column, and HPLC-grade tetrahydrofuran as an eluent at 40 °C), based on a calibration with polystyrene standards. The intrinsic viscosity−molecular weight relationship was obtained using an in-line configuration of a viscometer (Viscotek T60A, Houston, Texas) and SEC instrument. The CCD images were recorded on a Nikon Eclipse E400 fluorescence microscope equipped with a Nikon DL-5M digital camera. Photoluminescence spectra were measured on JASCO FP-6500 spectrofluorometers. The SEM image was recorded on an Hitachi S-3500N scanning electron microscope using an accelerating voltage of 20 kV. Transmission electron microscopy investigations were carried out with a JEOL JEM-3100FEF-3500N instrument.

Acknowledgment. We thank Profs. Hidenori Okuzaki at Yamanashi University, Kotohiro Nomura at Nara Institute of Science and Technology, and Kazuo Akagi at Kyoto University for fruitful discussions and helpful guidance. We are also grateful to Hirotoshi Furusho for technical assistance in performing SEM and TEM measurements. This research was supported by a Grant-in-Aid for Scientific Researches in a priority area "Super-Hierarchical Structures" (No. 446) from the Ministry of Education, Culture, Sports, Science and Technology, Japan. M.F. is acknowledged in part for a grant from the Ministry of Education, Science, Sports, and Culture of Japan, for a Grant-in-Aid for Scientific Research, "Design, Synthesis, Novel Functionality of Nanocircle and Nanorod Conjugating Macromolecules (16205017)". G.K. acknowledges support by Kyungpook National University Research Fund, 2006.

CM061719U